PROCEEDINGS OF SPIE

SPIEDigitalLibrary.org/conference-proceedings-of-spie

Retardation of the oxidation of aluminum thin films in low-oxygen and cryogenic environments

Hart, S. Merlin, Smith, Donovan, Allred, David

S. Merlin Hart, Donovan K. Smith, David D. Allred, "Retardation of the oxidation of aluminum thin films in low-oxygen and cryogenic environments," Proc. SPIE 11451, Advances in Optical and Mechanical Technologies for Telescopes and Instrumentation IV, 1145149 (13 December 2020); doi: 10.1117/12.2576339

SPIE.

Event: SPIE Astronomical Telescopes + Instrumentation, 2020, Online Only

Downloaded From: https://www.spiedigitallibrary.org/conference-proceedings-of-spie on 08 Jan 2021 Terms of Use: https://www.spiedigitallibrary.org/terms-of-use

Retardation of the oxidation of aluminum thin films in low-oxygen and cryogenic environments

S. Merlin Hart*, Donovan K. Smith, and David D. Allred
Department of Physics and Astronomy, Brigham Young University, Provo, UT USA 84604
*samuelmerlinhart@gmail.com phone: 509-438-0367

ABSTRACT

Aluminum is the best choice of material for broadband mirrors. However, once an oxide layer forms on the surface of the mirrors the reflectance in the far ultraviolet range decreases. The study of Al mirrors is difficult because they oxidize so quickly in the air. This makes reproducibility and joint work between laboratories difficult because the mirrors will oxidize and make successive measurements inaccurate. We have found that storing aluminum thin-film mirrors in low oxygen environments (such as liquid nitrogen, dry ice, and hexane) retards mirror oxidation. We examined the retardation of the growth of aluminum oxide during storage in these environments. This oxidation retardation was most pronounced when mirrors were stored in liquid nitrogen. In comparing the growth rate of oxide out of storage to that while it was in storage, we found that the apparent growth of aluminum oxide, is 1/500 in liquid nitrogen, 1/200 in hexane and 1/40 in dry ice.

Keywords: mirror storage, space telescope mirror, far ultraviolet, spectroscopic ellipsometry, oxidation, longevity.

1. INTRODUCTION

Aluminum (Al) is the most promising candidate for next generation, broadband mirrors because of its unmatched high reflectance from deep ultraviolet (DUV), through the visible and infrared (IR) wavelengths. Two of NASA's upcoming projects, the Large UV/Optical/IR Surveyor (LUVOIR) and the Habitable Exoplanet Observatory (HabEx), depend on being able to observe a wide spectrum of electromagnetic radiation. More specifically, these two projects need mirrors that are able to observe into the Lyman Ultraviolet range (LUV, 91.2 nm – 121.6 nm). Current mirror technology on the Hubble Space Telescope (HST) uses a magnesium fluoride (MgF_2) protective layer over the Al which keeps the reflectance above 115 nm high but causes Al's reflectance to drop to around 15% at wavelengths below 110 nm [1]. Metal fluoride protective layers are used to prevent oxidation of the aluminum, but each has a characteristic wavelength below which they are opaque.

These protective layers are used to combat the formation of aluminum oxide which occurs rapidly when Al is exposed to the atmosphere of Earth. Even a thin layer of oxide decreases the Al mirror's reflectance in the UV range. It can be calculated that even a 1 nm layer of Al_2O_3 will decrease the reflectance of the mirrors from 90% (unoxidized) to 20% (1 nm) below 150nm [2]. This is an issue because before the mirrors are launched into space with the space telescope, they will be stored in air for long periods of time. Thus, they will necessarily have protective fluoride overcoats. But how thick must those overcoats be? Our group has experience in studying the oxidation of aluminum under ultrathin fluoride coatings, particularly aluminum fluoride (AlF_3). [2-4] If ultrathin fluoride films could be made sufficiently perfect they might be suitable for LUV applications. [5], [6] However, at the present the aluminum under such coatings does oxidize, albeit at a much slower rate than bare aluminum. It would be helpful to find ways to store samples for the purpose of shipping them from one lab to another without them changing significantly and to store them in the lab for future reference. We sought various storage environments which will dramatically arrest oxide growth on bare Al and AlF_3-coated mirrors. The environments studied were: liquid nitrogen (LN2) , hexane, dry ice and dry laboratory air (dew point < 273K). Another intent of this study is to understand the growth kinetics of Al_2O_3 on bare Al and under a protective fluoride layer. Because the retardation of oxidation in LN2 turned out to be so large we could not easily interpret the changes observed via spectroscopic ellipsometry (SE) for the AlF_3 on Al coatings stored in LN2. Bare Al

Advances in Optical and Mechanical Technologies for Telescopes and Instrumentation IV,
edited by Ramón Navarro, Roland Geyl, Proc. of SPIE Vol. 11451, 1145149
© 2020 SPIE · CCC code: 0277-786X/20/$21 · doi: 10.1117/12.2576339

Downloaded From: https://www.spiedigitallibrary.org/conference-proceedings-of-spie on 08 Jan 2021
Terms of Use: https://www.spiedigitallibrary.org/terms-of-use

samples were, therefore, used in this study so that we could have a better understanding of environmental ways of retarding oxide growth on the least complicated mirror surface before turning to coated mirrors.

.

2. EXPERIMENTAL METHODS

A breakdown of the methodology in creating and measuring the Al samples, analyzing the data and storage conditions.

2.1 Deposition of Al samples



Figure 1: Evaporation Chamber. 1. The insertion points for the evaporation boats. 2. The lower shutter that covers one boat while the other is depositing on the substrate. 3. The upper shutter that can be used to cover all of the samples on the deposition stage at once. 4. The thickness monitor.

The aluminum samples were deposited in a Veeco glass bell-jar thermal evaporator. Three independent, resistance-heated evaporation sources are arrayed horizontally at the bottom of the chamber which allows up to three different materials to be deposited without breaking vacuum. In our case, only the left source (see Fig. 1, left number 1) was used. The evaporator is equipped with an Inficon quartz-crystal thickness monitor (QCM) labelled 4 in Fig. 1 and two independent manual shutters used to control film thicknesses. A sample platen is located about 30 cm above the evaporation sources. The platen is drilled like an optical breadboard with threaded holes spaced an inch apart in a square pattern to facilitate the attachment of the downward-facing samples to its underside. No sample rotation occurs as the sample stage is fixed for the duration of the deposition. One shutter is placed immediately below the substrate platen (See Fig. 1 number 3). It is controlled by a vertical rod attached to a rotational feedthrough in the base plate. In its closed position it blocks atoms from all three sources, while in its open position, it allows atoms from all sources to the reach the samples attached to the bottom of the substrate platen.

The other shutter operates as an either/or shutter (see Fig. 1 number 2), allowing either Al atoms from the Al source or atoms from the companion source to strike the samples. In the figure the shutter is vertical. It would not be utilized in this position. This shutter is placed between two deposition sources, its axis horizontal and parallel to the long direction of the two sources and in the plane of the two sources. Its axis is attached to a rotation feedthrough that went through the aluminum collar ring that formed a portion of the bottom of the chamber. (The broad polished circular surface visible in

Downloaded From: https://www.spiedigitallibrary.org/conference-proceedings-of-spie on 08 Jan 2021
Terms of Use: https://www.spiedigitallibrary.org/terms-of-use

Fig. 1 is the collar's top surface). Aluminum was evaporated from 99.9% pure Al wire inserted in a tungsten coil (RD Mathis). The target Al evaporation rate was 3- 4 nm/sec. The chamber was evacuated to below $1x10^{-3}$ Pa before evaporation. Deposition took roughly 4 minutes.

The approximate 30mm by 30mm rectangular substrates were cleaved from a 200-mm-diameter Si (100) wafer coated with a nominal 300 nm of CVD Si_3N_4. The CVD Si_3N_4 dielectric layer on the substrate is referred to as the interference layer (IL). The cleaved samples were fixed directly to the 40-cm diameter sample platen with screws and washers.

2.2 Storage in liquid nitrogen *(*LN2), dry ice and hexane

After the deposition the samples were removed and measured on the JA Woollam Model M2000 variable-angle, spectroscopic ellipsometer (VASE). Then, some of the samples were stored in glass jars containing hexane and others were placed in a liquid nitrogen dewar. Each liquid nitrogen dewar held six dippers in it, which allowed for the easy storage and retrieval of specific samples without exposing other samples to the atmosphere. The dry ice storage consisted of an insulated cold shipping box in which the samples were stored between layers of dry ice, protected by lint free cloth. Each batch of samples that were created during the same run of the evaporator were labeled in storage so time in storage could easily be determined. Samples were removed from storage and measured via VASE and then left in lab conditions out of storage so that the samples could act as their own control sample. For each sample, we were able to compare the in-storage change in 'apparent' oxide thicknesses to the change in the sample with time while the sample was in ambient lab-air conditions.

Storing the samples in this way will give a clear picture of the differences between storage in cryo- and low-oxygen environments and storage in ambient air conditions at room temperature. Ambient lab air in our labs has a relative humidity of 18 to 22%, which corresponds to a dewpoint of 270 to 273K. The higher humidity levels were noted in summer and the lower ones in winter.

2.3 Ellipsometric characterization

After they were deposited, samples were measured with a J.A. Woollam M-2000D, variable-angle, spectroscopic ellipsometer (VASE) over the 190-1688 nm wavelength range. Ellipsometric reflectance data was then analyzed using the CompleteEASE® software from J.A. Woollam Company. The model used for analyzing the data is discussed below.

The top layer is the oxide layer. It is the thinnest of the layers since it is not deposited but grows from the oxidation of the aluminum layer. Since it is so thin, the first approach examined was to use literature constants for sapphire, also termed corundum. However, there are several reasons not to do so. The alumina that forms is likely not corundum/sapphire and can be expected to have optical constants significantly different. In fact, modeling with sapphire constants often produces an unphysically thick alumina layer. In addition, the apparent thicknesses would vary randomly for measurements made at different times on the same sample. On the other hand, if the optical constants and thickness are calculated for the layer as part of the as-deposited sample, those optical constants will produce consistent results for aging samples. Therefore, the Al_2O_3 was parameterized as a Cauchy layer, with fit parameters from previous work. However, the UV optical constants we not completely satisfactory so the modeled fits to the ellipsometric parameters: Psi and delta showed notable deviations at high wavelengths.

Under the alumina layer, lay the deposited Al film. The optical constants for thin-film metal layers like Al need to be treated differently than dielectrics because the behavior of their free electrons depends on film thickness, grain sizes and deposition conditions. This has long been known to be the case for aluminum [8] In this study, the Al layer was modeled as the sum of four to six Gaussian oscillators, a UV pole and the value of the dielectric constant at infinity. The parameters had been fixed from the study of an aluminum thin film as part of this study. The oscillator at zero eV corresponds to the free electron (Drude) contribution to aluminum's conductivity. The intensity and breadth of this oscillator varies with the thickness of the film and deposition conditions such as impurity concentration. We used the same aluminum model for each given sample, not adjusting the parameters values even as the sample aged. However, it was recognized that, an effective medium approximation (EMA) layer could be helpful to understand aging. Ultrathin aluminum films are known to have many grain boundaries, conceivably oxygen could penetrate along them, producing a small amount of oxide in the interior of the layer. We investigated this possibility by replacing the aluminum layer with an EMA layer composed of Al with voids and a small amount of aluminum oxide.

The Al we deposited onto our samples was thick enough to be opaque. That is, after 40 nm of Al, most of the light is absorbed. Some of our samples were around 40 nm thick and some were >80 nm thick. Due to the thickness of the Al,

Downloaded From: https://www.spiedigitallibrary.org/conference-proceedings-of-spie on 08 Jan 2021
Terms of Use: https://www.spiedigitallibrary.org/terms-of-use

the layers underneath did not affect our fitting process and were optical properties were held constant. These layers, in descending order, were 1nm silicon dioxide (SiO_2), 300 nm silicon nitride (Si_3N_4) and the silicon (Si) substrate.

For samples stored in hexane, for the purpose of fitting the ellipsometric data, we examined replacing the void material in the EMA layer with polyethylene, representing hexane, accounting for the possibility of hexane remaining in the samples by capillary action from their storage.

3. RESULTS AND DISCUSSION

It has been noted that that the growth in the apparent oxide thickness on aluminum slows down dramatically as the thickness of the oxide already on the film increases. Several approaches to parameterizing thickness with time-in-air have been examined for room temperature oxidation including, linear, parabolic, inverse-logarithmic (that is, Cabrera-Mott), and logarithmic. Al oxidation thickness increases linearly with the logarithm of time [4,8]. That is, when apparent thickness is plotted versus the logarithm of time, the thickness values lie more-or-less on a straight line.

The question we had was this: does storage in environments that are low oxygen, at reduced temperature or both, retard the oxidation during the time that it is stored? And secondly, is there a constant retardation factor or is the behavior more complicated? That is, suppose that after storage in a media for 100 hours that amount of oxidation is the same as one stored in air for 10 hours. If a similar sample is stored for twice as long in the ambient, will its in-storage oxidation have proceeded to the same extent as one stored in air for 20 hours? That would be a retardation factor.

This is the protocol for investigated the effect of storage conditions on the oxidation of bare Al samples: For any given sample, after storage for a long period of time with no disruptions, we removed the sample from storage, and measured it via VASE. Then the sample was not returned to storage. Instead it remained in lab air and was measured via VASE periodically as time went on. This provided a means to estimate the retardation in aging each individual sample may have enjoyed relative to one in air for the same time due to its storage in another environment. We could directly note the growth of the alumina, if any, while the sample was in storage and then compare it to the growth with time of the oxide which occurs later when the sample is stored in air. If the oxidation behavior of Al were affected by the deposition conditions doing this allowed the samples to act as their own control. In short, we were thus able to see how the surface film on each sample grew thicker first in the stored condition and later in the air.

We note that that in plotting the apparent thicknesses of the Al_2O_3 vs. the time since the sample deposition, there was a significant retardation in the logarithmic growth of the Al_2O_3 layer for the period of time that the sample was in storage. This result is most noticeable for the samples stored in LN2 for a long time (>3000 hours). Thus we know that there is retardation.

Considering now the experiments one-by-one:

3.1 Liquid nitrogen storage

We first plotted the apparent aluminum oxide thickness as a function of elapsed time since deposition, Figure 2. The thickness of the apparent oxide when the sample was first removed from the deposition chamber is less than one nanometer, blue dot on the left. This amount of oxide is not unexpected for a sample that was just deposited. The sample was then placed in liquid nitrogen for over 3000 hours before it was removed and placed in air. The points at the right are the measured thicknesses after it was removed and sat in air. the point of the left and those and the right do not lie on the same curve. The only way to make these show a coherent trend is to assume that oxidation did in fact slow down or cease while the sample was stored in LN2. Figure 3 shows the same data assuming that the 3343 hours in LN2 corresponded to no time at all. That is, when all of the time that the sample was in liquid nitrogen is counted as though it never happened, then the thicknesses with time appears to follow a logarithmic growth curve. While this is a better fit, it has two thicknesses for zero hours. This is clearly not true either.

Downloaded From: https://www.spiedigitallibrary.org/conference-proceedings-of-spie on 08 Jan 2021
Terms of Use: https://www.spiedigitallibrary.org/terms-of-use

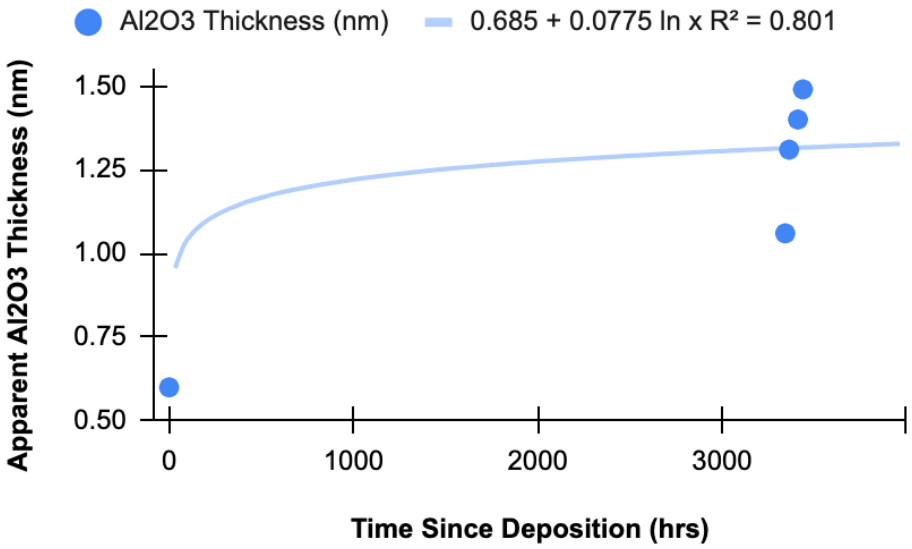


Figure 2. A plot of the apparent oxide thickness vs time since the Al was deposited on the substrate. The logarithmic curve here is to highlight that during the time in LN2 the growth of oxide was not the same as expected when in air. The growth of oxide spikes when the sample was taken out of the LN2 storage.

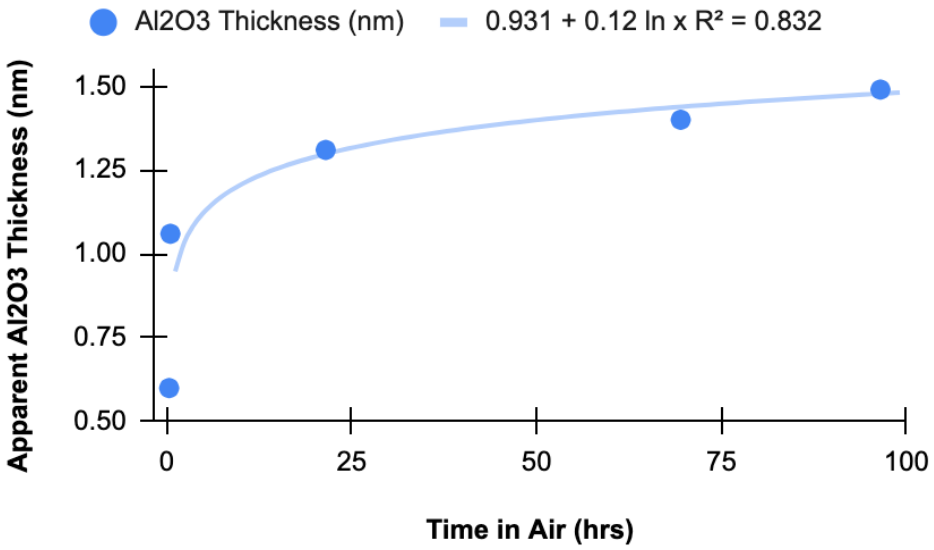


Figure 3. The data points on this graph are plotted as if during the time in LN2 the sample was in suspended animation. Meaning that the time spent in LN2 was effectively zero. This shows that having the time in LN2 be equal to almost no time in air allows the growth of oxide to fit a logarithmic growth curve much better.

Assuming that the change in the oxidation is logarithmic, for all measurements after the first, we subtracted from total time since deposition the amount of time that the sample had been in storage and added a constant time value such that the R^2 value was closest to 1, see figure 4. We found that the amount time spent in LN2, 3343 hours, was worth about 6 hours of air time. The value of time, 6 added to the air time of all of the points after storage was the amount of time that was most likely ”equal to” the amount of time that the sample spent in the LN2. Figure 4 is a graph of the R^2 values As a

Downloaded From: https://www.spiedigitallibrary.org/conference-proceedings-of-spie on 08 Jan 2021
Terms of Use: https://www.spiedigitallibrary.org/terms-of-use

function of the time adjustment value that we used. The R^2 value reaches a maximum of .996 the effective time in air is 6 hours. This is the value that we used in the calculation for the retardation factor from LN2 storage to air storage.

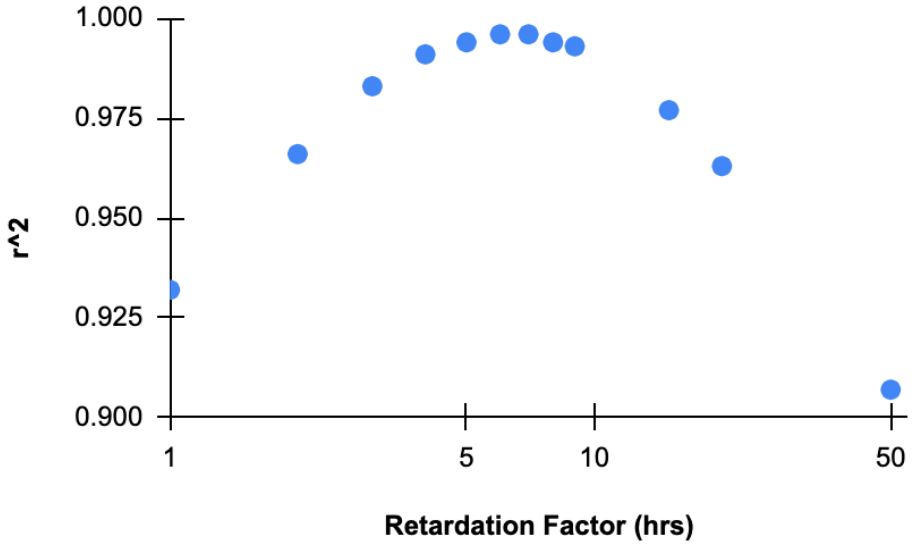


Figure 4. A plot of the R^2 values versus the effective time in air. The data has the best fit to a logarithmic curve when the effective time in air is 6 hours. Thus the retardation factor is 6/3343 which is around 1/500.

If we assume that the time that the sample was in LN2 corresponds to about 6 hours then the modeled thicknesses fall on the predicted thickness, which increases linearly with the log of time. Using a retardation factor of approximately 1/500, our fit had an R^2 (goodness of fit) value closest to 1.

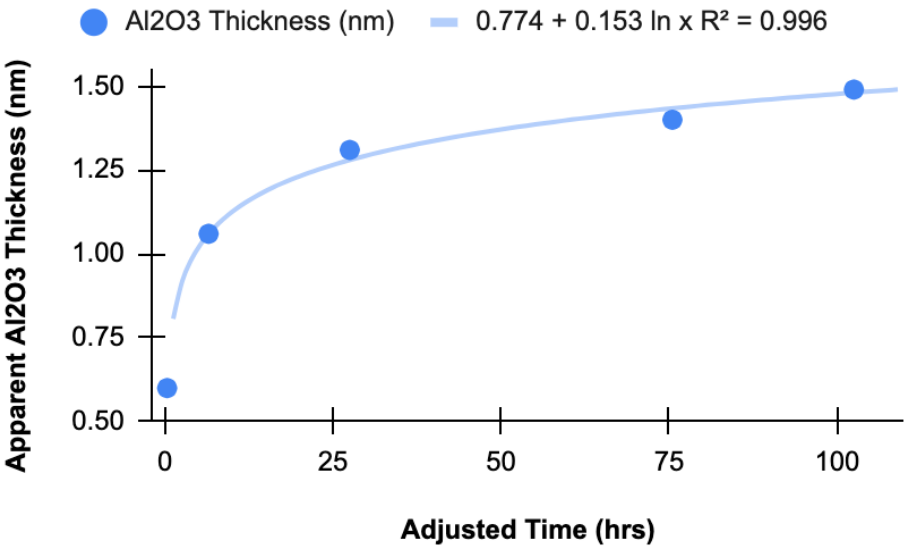


Figure 5. The time in LN2, 3343 hours turned into an effective 6 hours in air. Having a retardation factor of 1/500 for time in LN2 to time in air allows the data to be fit almost exactly, to a logarithmic curve. Showing that while oxidation does seem to happen during in LN2, it is at a much slower rate than in air.

Downloaded From: https://www.spiedigitallibrary.org/conference-proceedings-of-spie on 08 Jan 2021
Terms of Use: https://www.spiedigitallibrary.org/terms-of-use

While only the charts for the 200328B4 sample are shown here, the same trends were seen for the other samples stored in LN2. In figure 6 we plot the retardation time as found in this way vs the time that the sample spent in liquid nitrogen. The fact that these points lie on a straight line with an intercept very close to zero indicates that the concept of a retardation factor may have some validity. The slope of the graph is 2.14 x10^{-3}, meaning that the oxide grows in LN2 at about 1/500 the rate that it does in air on bare Al samples.

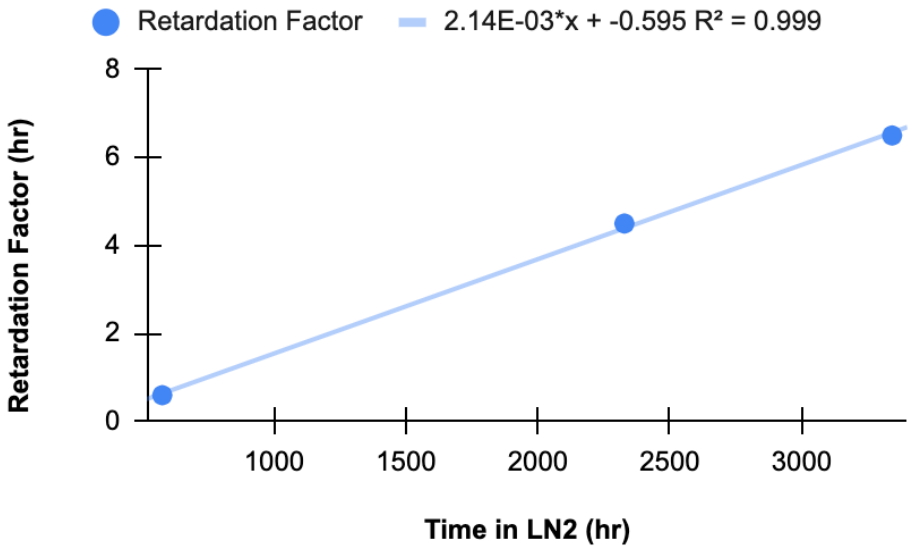


Figure 6. Retardation factor versus the amount of time that the sample was stored in liquid nitrogen. The slope of this graph gives a conversion factor between the time LN2 translates to time in air. The slope of the graph in this case is 2.14 x10^{-3} . Thus, the surface oxides grows in LN2 at about 1/500 the rate that it does in air.

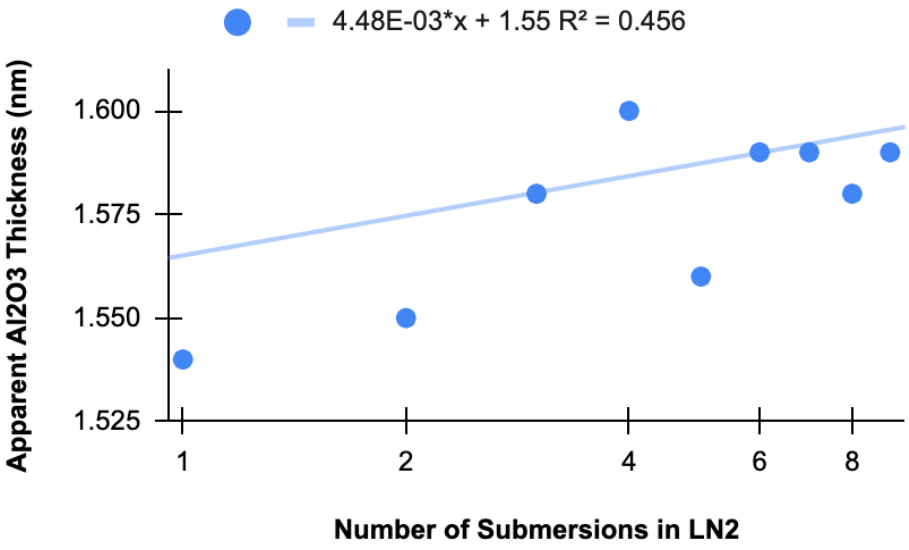


Figure 7. A plot of the apparent aluminum oxide thickness vs the number of times that the sample was submerged in LN2. This sample 200328 C4 had already been sitting in air for >3000 hours. It appears that the submersion of the sample in liquid nitrogen has an effect on the apparent thickness of the oxide layer.

Downloaded From: https://www.spiedigitallibrary.org/conference-proceedings-of-spie on 08 Jan 2021
Terms of Use: https://www.spiedigitallibrary.org/terms-of-use

We then looked for the effects of storage on the samples by submersing the samples in a storage condition for a short amount of time and then removing the sample immediately again to measure. Since it was possible that for samples stored in LN2, the thermal expansion and contraction of the sample when transitioning between room temperature (~300K) and liquid nitrogen temperature (77K) could result in microscopic deformations of the sample surface, we looked at the effect of repeated submersions in liquid nitrogen on the samples apparent Al_2O_3. We chose a surface that would likely not be change significantly between submersions from oxidation in the air: a sample that had already been in air for <3000 hours. Figure 7 shows that while there is a correlation between increased apparent oxide thickness with repeated exposure to the liquid nitrogen. Determining whether this effect is thermal or from condensation on the surface or something else will be the subject of later work.

3.2 Hexane storage

Are there liquids that at room temperature exclude water and/or oxygen? These are thought to be the two primary actors in the oxidation of aluminum. When placed in water hexane will not dissolve. Oxygen and water are both mostly insoluble in hexane. Thus, hexane is a candidate room temperature medium that may retard aluminum oxidation. Different bare aluminum samples were stored in the hydrocarbon hexane (C_6H_{14}) at room temperature to study the effects of storage in a low-oxygen environment at room temperature. The samples that were stored in hexane were treated as those in LN2. Sample 200328 C4 was stored in hexane for 1824 hours; then it was removed, measured and left in air for subsequent VASE measurements. The thickness versus time analysis was then done in the same way was done for the LN2 samples as explained above.

Figure 8 shows that there is a retardation effect is similar to that of liquid nitrogen, but less pronounced. Figure 9 shows the best fit curve for the 1824 hours in hexane is equivalent to about 9 hours in air. This is 0.5% of the time that it was in hexane, meaning for every 100 hours in hexane, it is equivalent to about 0.5 hours in air. This is a significant reduction in the rate of "oxide" growth, compared to the rate at which it oxidizes in air. Storage in hexane is an effective way to retard the growth of "oxide" but not quite as effective as liquid nitrogen.

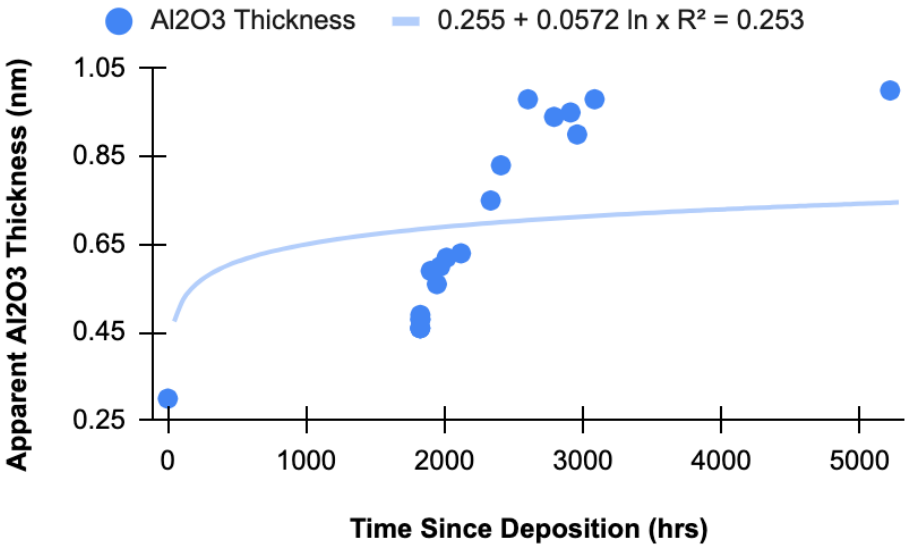


Figure 8. From looking at the data points for apparent oxide growth for the sample that has been stored in hexane it is clear that the storage time in hexane reduced the amount of oxide growth during that time by a significant amount since it does not follow the logarithmic curve.

Downloaded From: https://www.spiedigitallibrary.org/conference-proceedings-of-spie on 08 Jan 2021
Terms of Use: https://www.spiedigitallibrary.org/terms-of-use

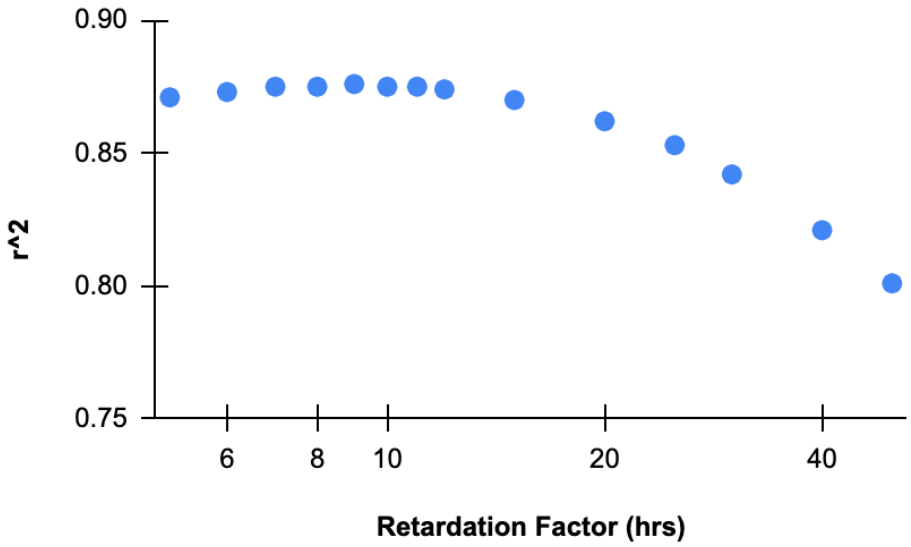


Figure 9. The retardation factor multiplied by the time spent in storage, which allows us to plot time on the x axis. The data fits most closely to a logarithmic curve at 9 hours, though the peak is approximately the same from 7-11. Using the best fit of 9 effective hours in air, that gives a retardation factor of 9/1824 or about 1/200.

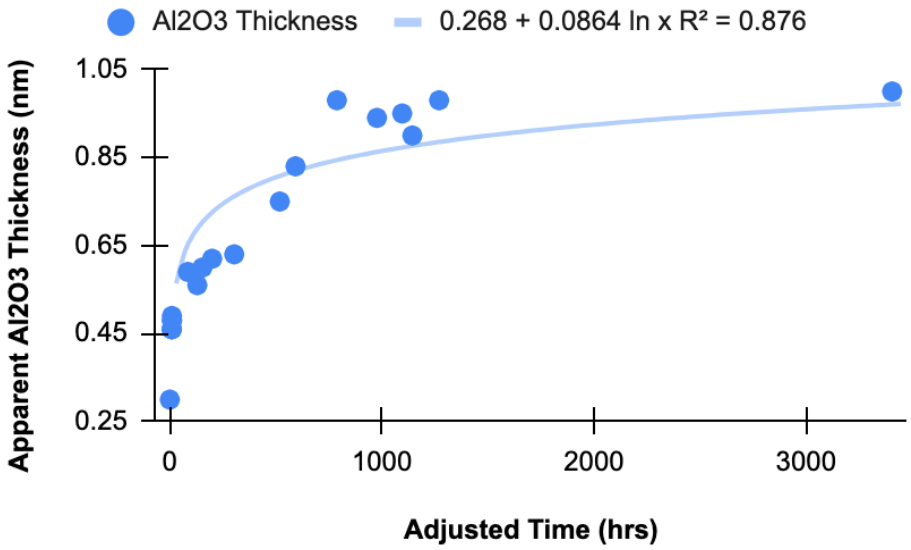


Figure 10. Adjusted time in hexane: For this data set, the 1824 hours in hexane was reduced to an equivalent 35 hours in air. The time between measurements is then added this adjusted time. This is a much better fit than if the time in hexane is assumed to be the same as air (compare to figure 8). Though the fit is not as good as observed for samples stored in LN2.

3.3 Oxidation in air

Figure 11 shows that the oxidation of our samples follows the logarithmic trend. All samples were measured prior to being put in storage. This gave us a starting point from which we could base each sample of off. Each samples started with different amounts of oxide. Each data set shows a clear logarithmic trend once it was exposed to air, though the

Downloaded From: https://www.spiedigitallibrary.org/conference-proceedings-of-spie on 08 Jan 2021
Terms of Use: https://www.spiedigitallibrary.org/terms-of-use

individual differences in the amounts of oxide on each film can be explained by differences is the compositions of the films.

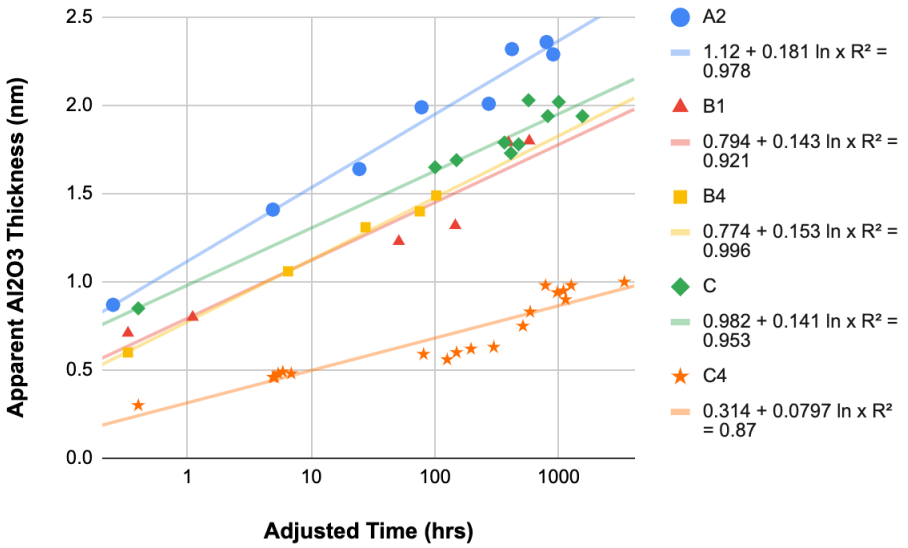


Figure 11. This shows the growths apparent aluminum oxide on several samples in air. The first point on each graph is prior to storage, and the method described above of including a retardation factor has been used for each of these samples to find a growth rate of the oxide in air.

3.4 Storage in dry ice

Sending samples stored in LN2 or hexane across the country to be analyzed at a different lab is quite difficult. Pressurized containers are dangerous and an open container is subject to spilling. This led us to investigate the viability of using dry ice to slow the rate of growth "Al_2O_3" in our samples, because dry ice can be used in shipping and will not spill easily. Our sample was stored in LN2 for 2928 hours before we took it out and placed it in dry ice storage.

Our dry ice sample was placed into a dry ice shipping box. The sample was sandwiched between dry ice, with newspaper and lint free cloth isolating the sample from contact with the dry ice. Every two to three days the dry ice was replaced. The sample was kept as cold as possible during the refills and the refilling process was done as fast as possible. The sample was exposed to the atmosphere for less than 2 minutes each time the dry ice was replaced, but was not given the opportunity to warm up. Only a few data points were collected for the dry ice storage because it was exposed to air over a weekend when all the dry ice sublimated. Data taken for this dry ice sample was different than the others. VASE measurements were taken during the storage process. This means sample was taken from storage, measured and then put back in storage.

Downloaded From: https://www.spiedigitallibrary.org/conference-proceedings-of-spie on 08 Jan 2021
Terms of Use: https://www.spiedigitallibrary.org/terms-of-use

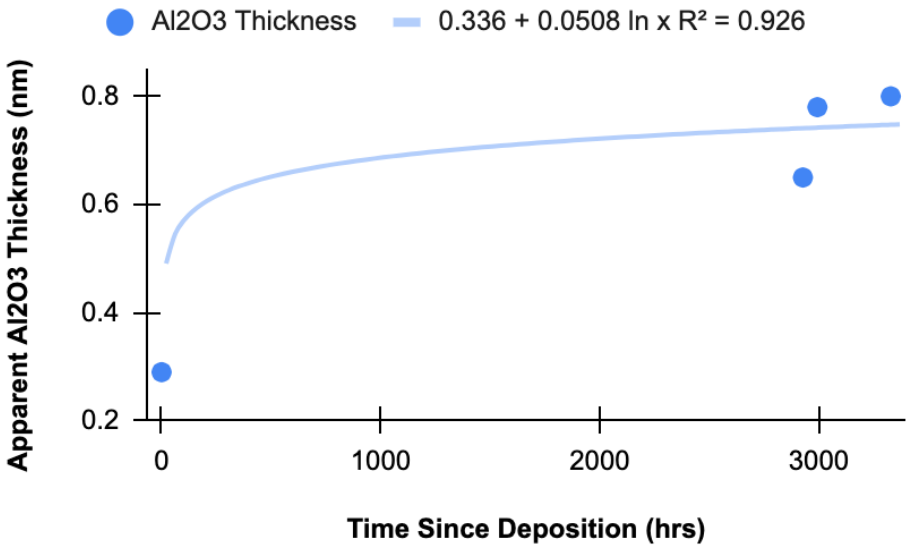


Figure 12. This graph shows the apparent thickness of Al_2O_3 as measured from deposition. The 2928 hours in LN2 and 335 hours in dry ice have not been adjusted for equivalent time in air.

As seen in figure 12, the data does not fit well when the time in storage is not changed by a retardation factor. Since sample was stored in two different mediums, two different retardation factors were used to fit the data to a logarithmic curve. In figure 13, the time in LN2 has been adjusted from 2928 hours to 5.86 hours in accordance to our findings in earlier for the ratio of oxidation growth in LN2 vs air for bare Al (see section 3.1). With the time in LN2 adjusted accordingly, we then found the retardation factor for the dry ice. Figure 13 shows the R^2 values when the retardation factor of the dry ice is change. The best fit occurs when the time in CO_2 is 0.025 apparent hours in air /1 hour in CO_2.

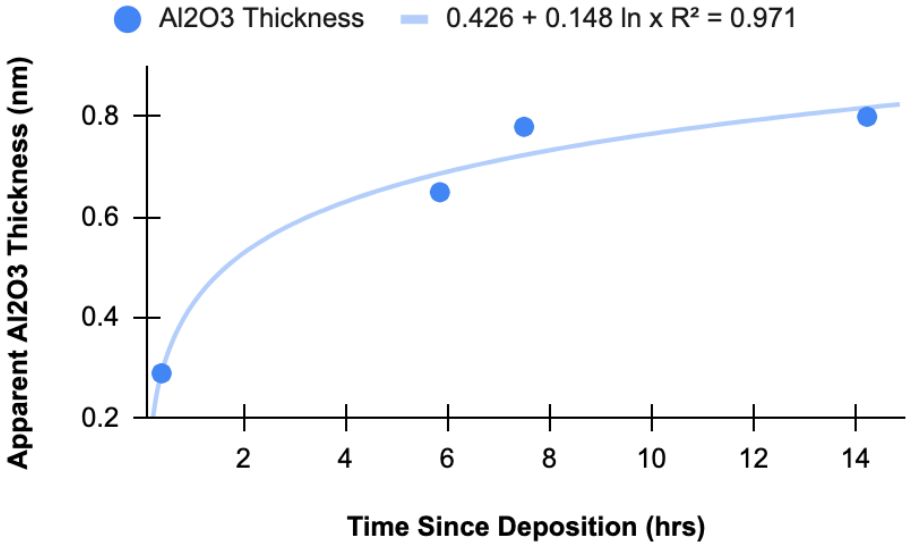


Figure 13. This graph shows the best fit curve for our sample that was stored in both LN2 and dry ice. The 2928 hours in LN2 was adjusted to 5.85 hours which is 1/500 of the time, based on our findings for oxide growth in LN2. The best fit occurred when the oxidation rate in dry ice is 2.5/100 as opposed to oxide growth in air.

Downloaded From: https://www.spiedigitallibrary.org/conference-proceedings-of-spie on 08 Jan 2021
Terms of Use: https://www.spiedigitallibrary.org/terms-of-use

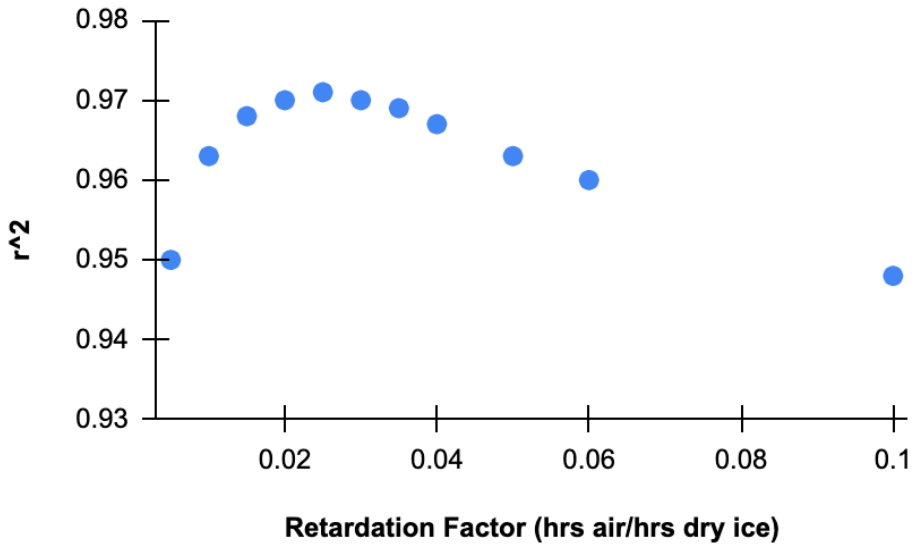


Figure 14. This shows the R^2 value on the y axis and the equivalent ratio of apparent air / time dry ice on the x-axis. The best fit happens when the equivalent time in air is 2.5% of the time spent in dry ice storage.

4. SUMMARY AND CONCLUSION

Our data shows that the storage of Al mirrors in these low oxygen / cryogenic environments significantly retards the growth of oxide on aluminum and we quantified this retardation. By comparing the amount of oxide growth on several films in each of the environments, we saw that the oxide growth is retarded by a constant factor for each medium. Variable-angle, spectroscopic ellipsometry was used to do this. We were able to model the apparent growth of aluminum oxide on aluminum thin films. We compared the growth of this oxide in liquid nitrogen, hexane, and dry ice to the growth rate in air. As compared with the growth of apparent aluminum oxide in air, the rate in liquid nitrogen is 1/500, the growth in hexane is 1/200 and the rate on dry ice is 1/40. We term this the retardation factor.

Additionally, storage itself is shown to have a small effect on the apparent thickness of the films. The apparent oxide tends to increase with repeated exposure to liquid nitrogen. This study contributes to the body of knowledge on preservation of aluminum mirrors, by bringing forward some ways in which oxidation of aluminum can be slowed. This opens up further study in long term storage of aluminum thin films without the growth of oxide.

ACKNOWLEDGEMENTS

We would like to thank these Brigham Young University personnel: R. Steven Turley for helpful suggestions in understanding data, Matt Linford for assistance with SE, and John Ellsworth with help on the evaporator used here. This paper would not have been possible without their help and support. Merlin Hart and Donovan Smith were supported by the College of Physical and Mathematical Science at Brigham Young University. We further thank our loved ones for believing in us and supporting us in this endeavor.

Downloaded From: https://www.spiedigitallibrary.org/conference-proceedings-of-spie on 08 Jan 2021
Terms of Use: https://www.spiedigitallibrary.org/terms-of-use

REFERENCES

[1] Fleming, B., Quijada, M., Hennessy, J., Egan, A., Del Hoyo, J., Hicks, B. A., Wiley, J., Kruczek, N., Erickson, N., and France, K., "Advanced environmentally resistant lithium fluoride mirror coatings for the next generation of broadband space observatories," Appl. Opt. 56, 9941-9950 (2017).

[2] Davis, A. A. “Oxidation of Aluminum Under Various Thicknesses of Aluminum Fluoride” B.S Thesis. Brigham Young University, 2018.

[3] Miles, M. “Evaporated Aluminum Fluoride as a barrier Layer to Retard Oxidation of Aluminum Mirrors” Theses and Dissertations, BYU. 6630 (2017)

[4] Allred, D. D., Turley, R. S., Thomas, S. M., Willett, S. G., Greenberg, M. J., And Perry, S. B., “Adding EUV reflectance to aluminum-coated mirrors for space-based observation," Proc. SPIE 10398, 34 (2017

[5] Hennessy, J., Balasubramanian, K., Moore, C. S., Jewell, A. D., Nikzad, S., France, K., & Quijada, M. (2016). Performance and prospects of far ultraviolet aluminum mirrors protected by atomic layer deposition. *Journal of Astronomical Telescopes, Instruments, and Systems*, *2*(4), 041206. https://doi.org/10.1117/1.jatis.2.4.041206

[6] Egan, A., Fleming, B. T., Wiley, J., Quijada, M., Del Hoyo, J., Hennessy, J., Hicks, B., France, K., Kruczek, N., Erickson, N., "The development and characterization of advanced broadband mirror coatings for the far-UV," Proc. SPIE 10397, UV, X-Ray, and Gamma-Ray Space Instrumentation for Astronomy XX, 1039715 (31 August 2017); https://doi.org/10.1117/12.2274141

[7] Nguyen, H. V., An, I., Collins, R W., “Evolution of the optical functions of thin-film aluminum: A real-time spectroscopic ellipsometry study,” Physical Review B 47, 3947 (1993).

[8] Grimblot, J. "II. Oxidation of Al Films," J. Electrochem. Soc. 129(10), 2369 (1982).

Downloaded From: https://www.spiedigitallibrary.org/conference-proceedings-of-spie on 08 Jan 2021
Terms of Use: https://www.spiedigitallibrary.org/terms-of-use